

The observation of structure in the dependence of the 1 keV positron backscattering coefficient on target atomic number

This article has been downloaded from IOPscience. Please scroll down to see the full text article.

1995 J. Phys.: Condens. Matter 7 3485

(<http://iopscience.iop.org/0953-8984/7/18/012>)

View [the table of contents for this issue](#), or go to the [journal homepage](#) for more

Download details:

IP Address: 171.66.16.179

The article was downloaded on 13/05/2010 at 13:04

Please note that [terms and conditions apply](#).

# The observation of structure in the dependence of the 1 keV positron backscattering coefficient on target atomic number

A P Knights† and P G Coleman

School of Physics, University of East Anglia, Norwich NR4 7TJ, UK

Received 6 January 1995

**Abstract.** The total backscattering coefficient  $\eta_+$  has been measured for 1 keV positrons incident normally on a number of elemental targets with atomic numbers  $Z$  in the range 6–82. The measurements require the minimization of surface contamination on the samples and as a result data analysis has to allow for the formation of positronium at the sample surface. Pronounced structure in  $\eta_+(Z)$  is observed, and it is suggested that this may be correlated with the effective atomic electron density.

## 1. Introduction

The first measurements of the total backscattering coefficients  $\eta_+$  of monoenergetic positrons, performed by Baker and Coleman in 1988 [1], have been followed by several studies of the backscattering of positrons from elemental solid surfaces [2–6]. In addition to their fundamental interest, a primary motivation for such studies has been the need to provide a stringent test for Monte Carlo simulations, which are used to predict positron implantation profiles and penetration depths necessary for the reliable analysis and interpretation of depth profiling data acquired by positron implantation spectroscopy. At present, good agreement has been observed between experiment and simulation for incident energies in the range 5–35 keV for total backscattering fractions and differential energy and angular spectra. In particular it has been shown that there is a smooth, monotonically increasing dependence of  $\eta_+$  on atomic number  $Z$  of the form  $Z^{1/2}$  at these incident energies.

Until now, the only low-incident-energy (i.e.  $\sim 1$  keV) measurements of positron backscattering have been performed under conditions where the possibility existed of their corruption by the presence of surface contamination [3, 5]. Low-incident-energy measurements are further complicated by the emission of positrons with work function or epithermal energies and those that leave the sample bound to an electron as positronium (Ps); any attempt to perform measurements of low-incident-energy backscattering has first to address these significant problems.

The study reported here has been performed on clean surfaces, and discriminates between positrons that are backscattered and those that are either thermalized and are re-emitted into the vacuum by the surface work function, or leave the surface at epithermal energies. The data analysis employed allows for the loss of positrons from the surface via the formation of Ps.

† Present address: Department of Physics, Royal Holloway, University of London, Egham, Surrey TW20 0EX, UK.

The results have been underpinned by the measurement of the spectrum of the effective perpendicular energies ( $P_p^2/2m$ , where  $P_p$  is the component of momentum perpendicular to the exit surface) of positrons backscattered from a polycrystalline Cu surface and its comparison with the Monte Carlo simulations of Jensen and Walker [7] and Ghosh and Aers [8].

## 2. Experimental set-up

The measurements were performed on the UEA magnetic transport beam, which is described elsewhere [9]. The experimental arrangement was described in detail by Coleman *et al* [5]; a 72% HPGe detector was used to measure the annihilation gamma count rate from a sample, viewed through a 1 cm wide lead slit so that only annihilation events in the sample were detected. The signal:background ratio was maximized by using only the 0.511 MeV photopeak in the gamma energy spectrum. The sample chamber was evacuated to  $\sim 10^{-10}$  Torr. The samples were tilted by  $3^\circ$  towards the detector to avoid significant gamma-ray attenuation in the sample and holder; this was not expected to affect the measurements as it has been shown that  $\eta_+$  is essentially independent of incident angle below about  $30^\circ$  [5].

The shape and position of the incident beam was monitored before each measurement by raising the sample and observing the beam profile with a CEMA/phosphor screen assembly at the end of the beam line. The beam was  $\sim 4$  mm in diameter, compared to typical sample sizes of 25 mm square. The position of the sample holder was adjusted so that the beam would hit each sample centrally by viewing the shadow of the corner of the sample holder in the image of the beam.

The positrons initially passed through parallel  $E \times B$  plates and were deflected by at least one beam diameter. This ensured that backscattered positrons were deflected again and were not able to return to the sample.

The sample holder allowed *in situ* heating to 700 °C and electrical isolation of the samples. The high-purity polycrystalline samples were fixed to the holder one at a time with a  $25 \times 25 \times 1$  mm<sup>3</sup> piece of Be suspended below in good electrical but poor thermal contact.

Prior to installation some of the samples were chemically etched to remove native oxide layers according to the recipes of Glang and Gregor [10]. To achieve atomically clean surfaces, *in situ* cleaning in the form of 1.2 keV Ar<sup>+</sup> ion sputtering and/or heating in an atmosphere of O<sub>2</sub>, or heating alone, was performed. Auger electron spectroscopy was used to monitor the surface condition. The contaminants, principally carbon and persistent oxide, were removed successfully, with the exception of traces of oxide remaining on the Al, Ge, Sn and Sm surfaces.

The effects of the contamination cannot be quantitatively determined, although it can be assumed that the low atomic number of oxygen, compared to that of the contaminated samples, would lower the measured  $\eta_+$  if present in sufficient quantities. However, the simulations of Jensen and Walker [7] give mean implantation depths of a few tens of nanometres for 1 keV positrons, which would imply that the mean penetration depths of backscattered positrons are typically  $\sim 10$  nm [6]. It can be assumed that the fractions affected by trace residual contamination at depths well below 1 nm are negligible and that the measured backscattering coefficients are a reasonably faithful representation of the true values.

### 3. Experimental method

In the ideal case where there is no work function or epithermal positron re-emission, or Ps formation, the gamma count rate  $N$  is simply proportional to the total number of positrons *not* backscattered from the sample. Then  $\eta_+ = 1 - N/N_0$ , where  $N_0$  is the count rate associated with the incident positron beam measured under the same experimental conditions.  $N_0$  is found by replacing the sample with the beryllium square and assuming  $\eta_+(\text{Be}) \approx 3.75\%$  [7]. However, while this ideal case is approximated by reality for high-energy ( $\geq 7$  keV) incident positrons, it does not describe adequately the conditions prevailing in the present experiment. We shall now consider the problems associated with low-energy backscattering measurements.

#### 3.1. Low-energy positron and Ps emission

Coleman *et al* [5] found evidence that surface contamination has a significant effect on the positron backscattering probability at low incident energies; it is therefore necessary to ensure that the sample surface is as clean as possible and that the experiment is performed in ultrahigh-vacuum (UHV) conditions. The combination of a clean surface and incident positron energy of 1 keV can, however, result in the emission of significant amounts of work function and epithermal positrons and of Ps. It is possible to return the re-emitted positrons to the sample by the application of a suitable negative potential—however, the neutral Ps can still escape. The relatively long-lived ortho-Ps (o-Ps) atoms can travel well beyond the volume viewed by the detector before (three-photon) annihilation occurs, and even then the gamma-ray energy is unlikely to lie within the 511 keV photopeak. Significant Ps formation, if not properly accounted for, leads to a reduction in the signal count rate and consequently an overestimation of  $\eta_+$ . Ps may be formed by the initial interaction of the primary beam and by re-emitted (or backscattered) positrons returned by the sample potential. It is possible in principle to measure separately the fraction of Ps formed at a sample surface by preventing the escape of *all* positrons, including those that are backscattered, by the application of the accelerating potential not as +1 kV to the primary source of the positron beam, but as -1 kV to the sample. Having determined the loss in gamma count rate due to Ps formation, a correction can be made to the original measurement and a value for  $\eta_+$  obtained.

#### 3.2. The separation of backscattered and epithermally emitted positrons

It is necessary to distinguish backscattered positrons from those that are re-emitted with work function or epithermal energies. In previous studies an arbitrarily chosen upper limit on the energy of the latter positrons in the region 20–50 eV has been found to be adequate. However, at an incident energy of 1 keV a more accurate method for discriminating between the two classes of positrons is required, as a significant number of positrons may be backscattered with energies of only a few tens of electronvolts.

Figure 1 shows plots of the annihilation gamma count rate from a clean polycrystalline Cu sample and the Be sample, bombarded by 1 keV positrons, measured as an applied sample potential was ramped from +10 V to -40 V. The count rate from the Cu sample exhibits a sharp increase as the potential is ramped through zero, corresponding to emission consistent with a previously measured small negative positron work function [11]. A smaller increase is observed for the Be sample, resulting from the emission of epithermal positrons only. An enlarged view of the Cu data reveals that the probability of epithermal positron emission, as for the Be in figure 1 (indicated by an arrow), appears to become insignificant at  $\sim 15$  eV. It was decided therefore that in this study backscattered positrons would be defined as those that are emitted from all samples with perpendicular energies  $> 15$  eV.

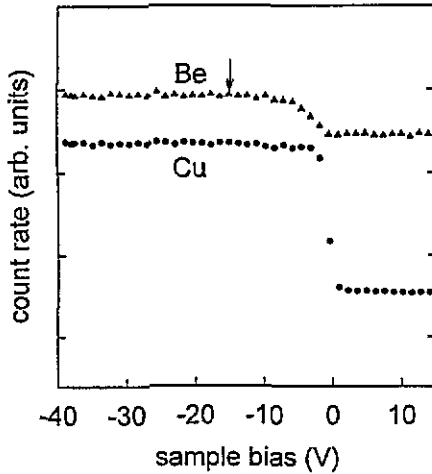


Figure 1. Integral perpendicular energy spectra of positrons re-emitted from Be (triangles) and Cu (circles) bombarded with 1 keV normally incident positrons. (See the text for definition of perpendicular energy.)

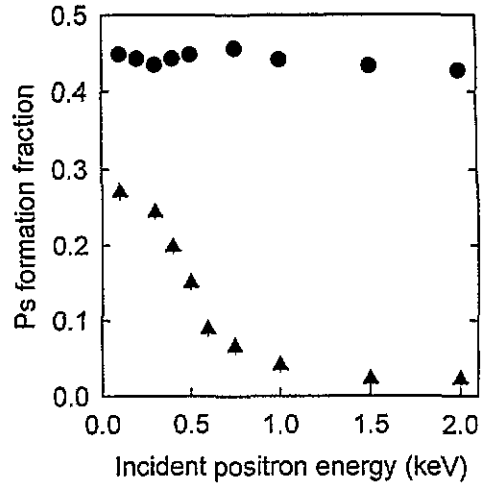


Figure 2. Ps formation fraction against incident positron energy for Cu (circles) and Be (triangles).

#### 4. Calculation of the backscattering coefficient $\eta_+$

With  $-15$  V applied to the sample and  $985$  V applied to the moderator (the primary slow positron source) the measured count rates from the sample under study and from the Be sample,  $N_{\text{sam}}$  and  $N_{\text{Be}}$  respectively, are:

$$N_{\text{sam}} = (N_0 - N_{\text{bk}})(1 - F_{\text{sam}}) \quad (1)$$

and

$$N_{\text{Be}} = 0.9625N_0(1 - F_{\text{Be}}) \quad (2)$$

where  $N_0$  is the incident positron count rate,  $F$  is the fraction of the non-backscattered incident flux that forms o-Ps at the surface and leaves the viewed volume and  $N_{\text{bk}}$  is the number of positrons backscattered from the sample (for Be,  $N_{\text{bk}} = 0.0375N_0$  at all energies).  $F$  includes re-emitted (work function or epithermal) positrons that are returned—possible more than once—to the sample by the applied negative bias and consequently form o-Ps; it is implied here that all returned slow positrons eventually either leave as o-Ps or are annihilated at the surface. The short-lived p-Ps atoms decay within the viewed volume and are therefore treated as surface annihilations for the purposes of this analysis.

With  $-1000$  V applied to the sample and  $0$  V applied to the moderator, the measured count rates are

$$N'_{\text{sam}} = (N'_0 - N'_{\text{bk}})(1 - F_{\text{sam}}) + N'_{\text{bk}}(1 - \beta_{\text{sam}}) \quad (3)$$

and

$$N'_{\text{Be}} = 0.9625N'_0(1 - F_{\text{Be}}) + N'_{\text{Bcbk}}(1 - \beta_{\text{Be}}) \quad (4)$$

where  $\beta$  refers to the fraction of backscattered positrons that eventually form o-Ps. The prime indicates that the counts are measured with 0 V applied to the moderator;  $N'_0 \neq N_0$  because in the two cases beams of very different energies are being transported along the beam axis towards the sample.

The fractions  $F$  and  $\beta$  may be determined by the relatively simple method used by Mills [12] and others to measure the Ps fraction  $F_{Ps}$ , based on a comparison of the area of the total annihilation gamma spectrum with the area of the photopeak only, with  $-15$  V on the sample. The measurement is made absolute by determining the ratio of areas under conditions for which  $F_{Ps} = 0$  (30 keV positrons incident on Be) and 100% (50 eV positrons on a negatively biased sample at high temperature).  $F_{sam} (= F_{o-Ps}) = 0.75F_{Ps}$  at 1 keV;  $\beta_{sam} = 0.75F_{Ps}$  at low incident energies; this is because the majority of the backscattered positrons are returned to the sample with perpendicular energies in the range of a few tens to a few hundred electronvolts.

Figure 2 shows the measured  $F_{Ps}$  versus incident energy for the polycrystalline Be and Cu samples. The uncertainty in  $F_{Ps}$  is typically 2.5%, which includes the uncertainty inherent in the calibration procedure. For Be it is assumed that the observed Ps formation is associated only with epithermal positrons because thermalized positrons could not pass through the sputtered Be surface region. The results suggest that epithermal emission in this case becomes negligible above an incident energy of 1 keV. Ps formation by non-thermalized positrons has been reported previously by Howell *et al* [13]. From the data of figure 2  $F_{Be} = 3.3\%$  and  $\beta_{Be} = 20\%$ , the latter being the low-energy asymptotic value of  $F_{Ps}$ .

Only  $\beta_{sam}$  is required for samples other than Be, as will be shown below.  $F_{Ps}$  for clean polycrystalline Cu is constant at 44% (i.e.  $\beta_{Cu} = 33\%$ ) within uncertainties for the incident energies shown. This value is in reasonable agreement with earlier measurements on single-crystal Cu (see, e.g., [14]). In contrast to the Be sample, the Cu was not ion sputtered but was cleaned by heating at 600 °C for 2700 s in an atmosphere of  $10^{-6}$  Torr  $O_2$ . Thermalized positrons can diffuse to the surface and form Ps there, so that a constant  $F$  over the range of incident energies shown is not surprising. For samples that, like Cu, were cleaned by heating processes,  $F_{Ps}$  is approximately constant between 100 eV and 1 keV, so that  $\beta_{sam} = 0.75F_{Ps}$ —whereas for samples that were ion sputtered an energy dependence of  $F_{Ps}$  similar to that for Be led to the adoption values of  $\beta_{sam}$  between 10 and 30%.

With knowledge of  $\beta_{sam}$ ,  $\beta_{Be}$  and  $F_{Be}$  one can evaluate the backscattering coefficient from equations (1)–(4) as follows. Equations (2) and (4) yield  $N_{Be} = 0.934N_0$  and  $N'_{Be} = 0.964N'_0$ , so that one may define  $\alpha$  as

$$\alpha = N_0/N'_0 = 1.032(N_{Be}/N'_{Be}). \quad (5)$$

Equation (3) may then be rewritten, using equations (1) and (5),

$$N_{bk} = [\alpha N'_{sam} - N_{sam}]/(1 - \beta_{sam}) \quad (6)$$

and, using  $N_0 = N_{Be}/0.934$ , one arrives at

$$\eta_+ = N_{bk}/N_0 = 0.934(\alpha N'_{sam} - N_{sam})/N_{Be}(1 - \beta_{sam}). \quad (7)$$

The statistical uncertainty on the measured value of each backscattering coefficient is calculated to be typically 3%. Additional uncertainties result, in the main, from the measurements of  $\beta$ .

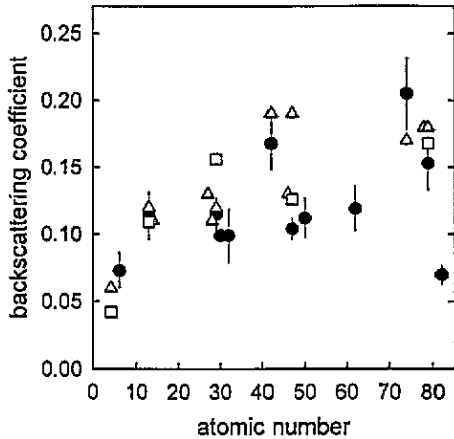


Figure 3. Total backscattered coefficient against target atomic number for 1 keV normally incident positrons: solid circles, present results; open squares, Monte Carlo results of Jensen and Walker [7]; open triangles, Monte Carlo results of Ghosh and Aers [8].

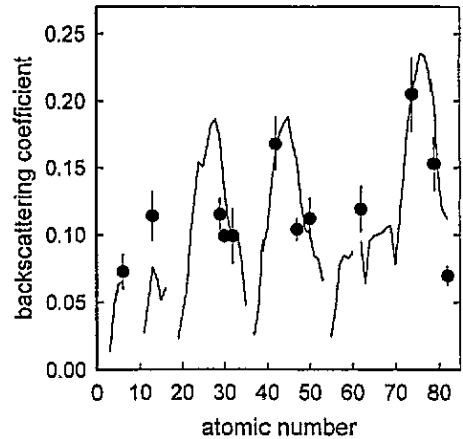


Figure 4. Total backscattered coefficient against target atomic number for 1 keV normally incident positrons: solid circles, present results; solid line, effective target electron density (normalized, but not fitted to the data; see the text for definition).

Table 1. Total backscattering coefficients for 1 keV incident positrons (uncertainties in parentheses).

Z	6	13	29	30	32	42
$\eta_+$ (%)	7.3(1.3)	11.4(1.8)	11.5(1.2)	9.9(0.5)	9.9(2.0)	16.8(2.0)
Z	47	50	62	74	79	82
$\eta_+$ (%)	10.4(0.8)	11.2(1.5)	11.9(1.7)	20.5(2.7)	15.3(2.0)	7.0(0.7)

## 5. Results

Figure 3 shows the results for  $\eta_+$  versus atomic number  $Z$  for 1 keV normally incident positrons together with the Monte Carlo simulation results of Jensen and Walker [7] and Ghosh and Aers [8]; the experimental data are listed in table 1.

Figure 4 shows the same experimental results plotted together with the normalized effective target electron density, where only electrons with binding energies  $< (1000/e)$  eV are considered; this will be discussed later.

## 6. Discussion

The backscattering coefficient  $\eta_+$  for 1 keV positrons clearly does not display the monotonically increasing dependence on  $Z$  observed in previous studies performed with higher-incident-energy particles, but instead exhibits a definite structure. The most striking individual result is that for Pb, which has a backscattering coefficient of 7%, less than half that obtained for Mo and smaller than that for Al.

Sternglass carried out a study of low-energy electron backscattering that suggested structure in the dependence of the total backscattering coefficient for electrons at low incident

energies [15]. Although the experiment was conducted in a vacuum of  $\sim 10^{-7}$  Torr and hence used contaminated surfaces, Sternglass was prompted to attribute the low-energy structure to the increasing importance played by inelastic scattering from target electrons in the backscattering process. He used the theory of inelastic collisions formulated by Bohr and Bethe [16] to show that only those target electrons that have velocities less than that of the incoming particle participate significantly in the scattering process, and that the maximum effectiveness of the scattering is reached when the target electrons have energies  $1/e$  that of the incoming particle. This criterion was used to obtain the plot of effective target electron density shown in figure 4. The structure of  $\eta_+$  versus  $Z$  and effective target electron density appear to be correlated, confirming the important role that positron–electron scattering plays not only in the slowing down of the positron but also in the backscattering process at an incident energy of 1 keV. The importance of this effect may well be different for incident positrons and electrons.

The most encouraging aspect of the present data is the successful comparisons that can be made with the Monte Carlo simulations of Jensen and Walker and Ghosh and Aers. The only serious discrepancy between the experimental data and the results of Jensen and Walker is for copper. Disagreement for Ag and W is found between the current data and the results of Ghosh and Aers. It is noted, however, that the two simulations disagree markedly for both Cu and Ag. Reasonable agreement is found with either one or both of the simulations for Al, Cu, Mo, Ag and Au.

## 7. Conclusions

Measurements of total backscattering coefficients  $\eta_+$  versus  $Z$  for 1 keV normally incident positrons have been presented. The measurements were performed on clean samples under UHV conditions with Ps formation being fully accounted for. The  $Z$  dependence of  $\eta_+$  is shown not to follow the smooth monotonic increase shown by other studies using positrons of higher incident energy, but exhibits a definite structure, which appears to be correlated with the effective target electron density. The results show reasonable agreement with the Monte Carlo simulation codes of Jensen and Walker and Ghosh and Aers.

## Acknowledgments

The authors would like to thank Dr A B Walker and Dr K O Jensen for many useful discussions, and Dr V Ghosh for sending us Monte Carlo simulation results prior to publication.

## References

- [1] Baker J A and Coleman P G 1988 *J. Phys. C: Solid State Phys.* **21** L875
- [2] Massoumi G R, Hozhabri N, Lennard W N and Schultz P J 1991 *Phys. Rev. B* **44** 3426
- [3] Mäkinen J, Palko S, Martikainen J and Hautojärvi P 1992 *J. Phys.: Condens. Matter* **4** L503
- [4] Massoumi G R, Hozhabri N, Jensen K O, Lennard W N, Lorenzo M S, Schultz P J and Walker A B 1992 *Phys. Rev. Lett.* **68** 3873
- [5] Coleman P G, Albrecht L, Jensen K O and Walker A B 1992 *J. Phys.: Condens. Matter* **4** 10311
- [6] Massoumi G R, Lennard W N, Schultz P J, Walker A B and Jensen K O 1993 *Phys. Rev. B* **47** 11007
- [7] Jensen K O and Walker A B 1993 *Surf. Sci.* **292** 83
- [8] Ghosh J V and Aers G C 1995 submitted



- [9] Hutchins S M, Coleman P G, Alam M A and West R N 1985 *Positron Annihilation* ed P C Jain, R M Singru and K P Gopinathan (Singapore: World Scientific) p 983
- [10] Glang R and Gregor L V 1970 *Handbook of Thin Film Technology* ed D Maissel and R Glang (New York: McGraw-Hill) ch 7
- [11] Schultz P J and Lynn K G 1988 *Rev. Mod. Phys.* **60** 748
- [12] Mills A P 1978 *Phys. Rev. Lett.* **41** 1828
- [13] Howell R H, Rosenberg I J and Fluss M J 1986 *Phys. Rev. B* **34** 3069
- [14] Lynn K G and Welch D O 1980 *Phys. Rev. B* **22** 99
- [15] Sternglass E J 1953 *Phys. Rev.* **95** 345
- [16] Bohr N 1913 *Phil. Mag.* **25** 10
- Bethe H A 1930 *Ann. Phys. Lpz.* **5** 325